 CMES, vol.105, no.6, pp.491-515, 2015

Numerical Solutions of Two-dimensional Stokes Flows by the Boundary Knot Method

Chia-Ming Fan[1,2], Yu-Kai Huang[1], Po-Wei Li[1] and Ying-Te Lee[1]

Abstract: In this paper, the boundary knot method (BKM) is adopted for accurately analyzing two-dimensional Stokes flows, dominated by viscous force and pressure gradient force. The Stokes flows, which denoted the flow fields with extremely viscous fluid or with very small velocity, appear in various engineering applications, such that it is very important to develop an efficient and accurate numerical method to solve the Stokes equations. The BKM, which can avoid the controversial fictitious boundary for sources, is an integral-free boundary-type meshless method and its solutions are expressed as linear combinations of non-singular general solutions for Stokes equations. The weighting coefficients in the solution expressions can be acquired by enforcing the satisfactions of boundary conditions at every boundary node, since the non-singular general solutions are derived in this paper and already satisfied the Stokes equations. Three examples of two-dimensional Stokes flows were adopted to validate the accuracy and the simplicity of the BKM. Besides, the optimal shape parameter in the non-singular general solutions was determined by examining the minimum average residual of the linear system from the BKM.

Keywords: Boundary knot method, two-dimensional Stokes flow, boundary-type meshless method, non-singular general solution, shape parameter.

1 Introduction

The Stokes flows, also known as the creeping flows or the low-Reynolds-number flows, are used to describe the flow fields, dominated by viscous force and pressure gradient force. Thus, the Stokes flows frequently appear in our daily life, such as the flow fields of honey and lubrication oil. The governing equations for Stokes flows, which are known as the primary-variable formulation, have been derived by

[1] Department of Harbor and River Engineering & Computation and Simulation Center, National Taiwan Ocean University, Keelung, Taiwan.
[2] Corresponding Author. E-mail: cmfan@ntou.edu.tw

following the conservation laws of mass and momentum. Because the computation of pressure component in the primary-variable formulation is non-trivial, different formulations of the Stokes equations have been developed, such as the velocity-vorticity formulation and the streamfunction formulation.

In the past decades, many numerical methods have been developed for numerical solutions of the primary-variable formulation [Barrero-Gil (2012); Zeb, Elliott, Ingham and Lesnic (1998)], the velocity-vorticity formulation [Young, Jane, Lin, Chiu and Chen (2004)] and the streamfunction formulation [Chen, Hsiao and Leu (2008); Young, Chiu, Fan, Tsai and Lin (2006)] in order to understand the underlying physics of the Stokes flows. For example, Zeb, Elliott, Ingham and Lesnic (1998) adopted the boundary element method (BEM) with the Stokeslets, the fundamental solutions of the Stokes equations, to analyze two-dimensional Stokes equations, while Young, Jane, Lin, Chiu and Chen (2004) used the radial basis function collocation method (RBFCM) to solve the velocity-vorticity formulation of the Stokes equations. Although some numerical schemes have been proposed to successfully solve different formulations of the Stokes equations, it is still essential to develop an accurate, reliable and simple numerical method for solutions of Stokes equations. In this paper, we proposed a novel boundary-type meshless method for accurately analyzing the primary-variable formulation of the Stokes equations.

Since computer technology has been rapidly developed in the past, many numerical methods have been proposed to analyze various partial differential equations and engineering applications. In comparison with the mesh-based methods, the developments of the so-called meshless (or meshfree) methods caught many researchers' attention, since the meshless methods can truly get rid of time-consuming mesh generation and numerical quadrature. During the past two decades, there are many promising meshless methods proposed, such as the method of fundamental solutions (MFS) [Alves and Silvestre (2004); Barrero-Gil (2013); Chen, Lee, Yu and Shieh (2009); Tsai and Young (2013); Young, Chen, Fan, Murugesan and Tsai (2005); Young, Jane, Fan, Murugesan and Tsai (2006)], the Trefftz method [Fan, Chan, Kuo and Yeih (2012); Karageorghis, Lesnic and Marin (2014); Ku (2014)], the singular boundary method (SBM) [Chen and Gu (2012); Chen, Fu and Wei (2009); Fu, Chen, Chen, Qu (2014)], the boundary knot method (BKM) [Canelas and Sensale (2010); Chen (2002); Chen and Hon (2003); Chen, Shen, Shen and Yuan (2005); Chen and Tanaka (2002); Hon and Chen (2003); Jin and Zheng (2005a); Jin and Zheng (2005b); Lin, Chen, Chen and Jiang (2013); Wang, Chen and Jiang (2010); Zhang and Wang (2012); Zheng and Ma (2012)], the method of approximate particular solutions (MAPS) [Chen, Fan and Wen (2011); Chen, Fan and Wen (2012)], the generalized finite difference method (GFDM) [Benito,

Urena, Gavete and Alonso (2008); Chan, Fan and Kuo (2013); Fan, Huang, Li and Chiu (2014)], the local RBFCM (LRBFCM) [Chan and Fan (2013); Fan, Chien, Chan and Chiu (2013); Vertnik and Sarler (2009)]. The MAPS, the GFDM and the LRBFCM are three promising domain-type meshless methods and can be applied to various partial differential equations. Since both of the interior nodes and the boundary nodes are needed in the implementations of these domain-type methods, the efficiency of numerical simulations by using the domain-type meshless methods is worse than the boundary-type meshless methods for some cases.

The MFS, the Trefftz method, the SBM and the BKM are four powerful boundary-type meshless methods. Since only boundary nodes are necessary for numerical simulations by using the boundary-type meshless methods, the dimensionality of the problem under consideration can be reduced by one and the efficiency of computer simulation can be greatly improved. The MFS remains the merits of the BEM, since it is involved from the BEM. The solutions in the MFS can be expressed by a linear combination of the fundamental solutions which are located out of the computational domain in order to avoid numerical singularity. By enforcing the satisfactions of boundary conditions at every boundary node, a system of linear (or non-linear) algebraic equations is yielded and the coefficients in the solution expression can be acquired by solving this resultant system. The MFS is very powerful if the fundamental solutions of the governing equations can be found. On the other hand, the accuracy of solution in the MFS is greatly influenced by the locations of fictitious boundary for fundamental solutions. In order to avoid the controversial fictitious boundary for fundamental solutions in the MFS, some relevant methods have been proposed, such as the SBM and the BKM.

In the BKM, the solution is expressed as a linear combination of non-singular general solutions instead of the fundamental solutions in the MFS. The sources in the BKM are located exactly on the physical boundary, such that the problem of fictitious boundary in the MFS can be eliminated. The BKM remains the merits of the MFS and, in the meantime, gets rid of the troublesome problem of the locations of sources. The BKM was proposed by Chen and Tanaka (2002) and then a symmetric BKM is also proposed by Chen (2002). Meanwhile, Chen, Chang, Chen and Chen (2002) and Chen, Chang, Chen and Lin (2002) also used the non-singular general solution to avoid possible numerical singularity of the MFS and successfully analyzed the eigenproblems in acoustics. During the past ten years, the BKM have been applied for various problems, such as Helmholtz equation [Chen and Hon (2003); Hon and Chen (2003)], Poisson equation [Chen, Shen, Shen and Yuan (2005)], inverse problems [Jin and Zheng (2005a); Jin and Zheng (2005b)], elastic and viscoelastic problems [Canelas and Sensale (2010)], and axisymmetric Helmholtz problems with high wavenumber [Lin, Chen, Chen and Jiang (2013)].

An overview of the BKM can be found in [Zhang and Wang (2012)]. Based on the above discussions of the BKM, it can be noticed that the BKM has been only used for numerical solutions of simple and single partial differential equation, except for the elastic and viscoelastic problems in [Canelas and Sensale (2010)]. In [Canelas and Sensale (2010)], it was the first time that the BKM is adopted for numerical solutions of vector equations. Thus, in this paper we would extend the BKM for numerical solutions of another system of vector equations, the Stokes equations, and the non-singular general solutions of the Stokes equations are also derived.

Like the fundamental solution in the MFS, we have to derive the non-singular general solutions of the Stokes equations if the BKM is adopted. The fundamental solutions for the Stokes equations are known as the Stokeslets [Alves and Silvestre (2004); Young, Chen, Fan, Murugesan and Tsai (2005); Young, Jane, Fan, Murugesan and Tsai (2006); Zeb, Elliott, Ingham and Lesnic (1998)], which can be derived by using the Hormander operator decomposition technique [Rashed (2002); Tsai and Hsu (2011)]. By carefully observing the mathematical derivation of the Stokeslets, it can be found that the fundamental solutions of the Stokes equations are represented by vector derivatives of a scalar potential. When two-dimensional Stokes equations are considered, the scalar potential is the fundamental solution of a bi-harmonic operator. Namely, the two-dimensional Stokeslets are expressed as vector derivatives of the fundamental solution of a bi-harmonic operator. Therefore, in this study, we adopted the non-singular general solution of bi-harmonic operator [Chen, Fu and Jin (2010)] to replace the fundamental solution of bi-harmonic operator during the mathematical derivation, such that the non-singular general solutions for the Stokes equations can be derived. Once the non-singular general solutions for the Stokes equations are obtained, the velocity components, pressure, vorticity and streamfunction can be expressed as linear combinations of the non-singular general solutions.

By enforcing the satisfactions of given linear boundary conditions at every boundary node, a system of linear algebraic equations is yielded and then the coefficients in the solutions expressions can be acquired by solving this resultant system. The solutions and their derivatives can be obtained by simple summation once the coefficients are acquired. The proposed BKM is very simple, accurate and easy-to-use when the Stokes equations are considered. Three examples were provided to verify the merits of the proposed boundary-type meshless method. The motivation of this study and the discussions of relevant literatures were provided in the first section. Then, the Stokes equations and the numerical procedures of the BKM were discussed. Followings were numerical results and comparisons. Finally, some conclusions and discussions were drawn.

2 Governing Equations for Stokes Flow

When the viscous force and the pressure gradient force dominate the flow fields in comparison with the inertial force, the flow fields are called the Stokes flows, which are also known as the creeping flows. The governing equations for Stokes flows can be derived by following the conservation laws of mass and momentum,

$$-\nabla^2 u + \frac{\partial p}{\partial x} = 0 \quad \mathbf{x} \in \Omega \tag{1}$$

$$-\nabla^2 v + \frac{\partial p}{\partial y} = 0 \quad \mathbf{x} \in \Omega \tag{2}$$

$$\frac{\partial u}{\partial x} + \frac{\partial v}{\partial y} = 0 \quad \mathbf{x} \in \Omega \tag{3}$$

where $u(\mathbf{x})$ and $v(\mathbf{x})$ are x-directional and y-directional velocity components, respectively. $p(\mathbf{x})$ is the pressure component, Ω is the computational domain, $\mathbf{x} = (x,y)$ is the space coordinates and $\nabla^2 = \frac{\partial^2}{\partial x^2} + \frac{\partial^2}{\partial y^2}$ is the Laplacian differential operator. Equations (1) and (2) are the x-directional and y-directional momentum equations as well as Eq. (3) is the continuity equation.

The above system of Eqs.(1)-(3) is known as the primary-variable formulation of the Stokes equations. Except for two velocity components and one pressure component, the vorticity and the streamfunction are also important to flow fields. The definitions for the vorticity and the streamfunction are shown as follows:

$$\omega = \frac{\partial v}{\partial x} - \frac{\partial u}{\partial y}, \tag{4}$$

$$u = \frac{\partial \psi}{\partial y}, \tag{5}$$

$$v = -\frac{\partial \psi}{\partial x}, \tag{6}$$

where $\omega(\mathbf{x})$ and $\psi(\mathbf{x})$ are the vorticity and the streamfunction. Once the Stokes equations, Eqs. (1)-(3), with suitable boundary conditions are solved numerically, the solutions of velocity components, pressure, vorticity and streamfunction can be acquired simultaneously. In this paper, we adopted the BKM, one kind of boundary-type meshless methods, to efficiently analyze the above Stokes equations.

3 Numerical Method

Since the solution in the BKM is expressed by linear combination of non-singular general solutions, we have to derive these non-singular general solutions for two-dimensional Stokes equations in this section. First, we adopted the Hormander operator decomposition technique [Rashed (2002); Tsai and Hsu (2011)] to derive the Stokeslets. During the mathematical derivations, it will be noticed that the fundamental solutions of the Stokes equations are expressed as vector derivatives of a scalar potential, which is the fundamental solution of bi-harmonic differential operator. Instead of using the fundamental solution of bi-harmonic operator, we adopted the non-singular general solution of bi-harmonic operator to acquire the non-singular general solutions of the Stokes equations.

In order to derive the non-singular general solutions of the Stokes equations, Eqs. (1)-(3) are re-written in the following matrix form:

$$\begin{bmatrix} -\nabla^2 & 0 & \frac{\partial}{\partial x} \\ 0 & -\nabla^2 & \frac{\partial}{\partial y} \\ \frac{\partial}{\partial x} & \frac{\partial}{\partial y} & 0 \end{bmatrix} \begin{Bmatrix} u \\ v \\ p \end{Bmatrix} = \tilde{L} \begin{Bmatrix} u \\ v \\ p \end{Bmatrix} = \begin{Bmatrix} 0 \\ 0 \\ 0 \end{Bmatrix}. \tag{7}$$

Then, we defined the fundamental solutions of the Stokes equations by the following equation,

$$\tilde{L} \begin{bmatrix} g_1^u & g_2^u & 0 \\ g_1^v & g_2^v & 0 \\ g_1^p & g_2^p & 0 \end{bmatrix} = \begin{bmatrix} -\delta(\mathbf{x}-\mathbf{s}) & 0 & 0 \\ 0 & -\delta(\mathbf{x}-\mathbf{s}) & 0 \\ 0 & 0 & 0 \end{bmatrix}, \tag{8}$$

where $\mathbf{s} = (s_x, s_y)$ and $\delta()$ are the space coordinates of source and the Dirac delta function. The adjoint operator of $\tilde{L}$ can be demonstrated as,

$$\tilde{L}^{adj} = \begin{bmatrix} -\frac{\partial^2}{\partial y^2} & \frac{\partial^2}{\partial x \partial y} & \left(\frac{\partial}{\partial x}\right)\nabla^2 \\ \frac{\partial^2}{\partial x \partial y} & -\frac{\partial^2}{\partial x^2} & \left(\frac{\partial}{\partial y}\right)\nabla^2 \\ \left(\frac{\partial}{\partial x}\right)\nabla^2 & \left(\frac{\partial}{\partial y}\right)\nabla^2 & \nabla^2\nabla^2 \end{bmatrix}, \tag{9}$$

which is defined by

$$\tilde{L}\tilde{L}^{adj} = \tilde{L}^{adj}\tilde{L} = \mathbf{I}\det(\tilde{L}) = \mathbf{I}\nabla^2\nabla^2, \tag{10}$$

where $\mathbf{I}$ is the identity matrix. According to the Hormander operator decomposition technique, a scalar function G is assumed such that

$$\begin{bmatrix} g_1^u & g_2^u & 0 \\ g_1^v & g_2^v & 0 \\ g_1^p & g_2^p & 0 \end{bmatrix} = \tilde{L}^{adj} \begin{bmatrix} G & 0 & 0 \\ 0 & G & 0 \\ 0 & 0 & 0 \end{bmatrix}. \tag{11}$$

Substituting Eq.(11) to Eq.(8) and using Eq. (10) will result in

$$\nabla^2\nabla^2 G = -\delta(\mathbf{x}-\mathbf{s}). \tag{12}$$

From the above equation, it is obvious that the scalar function G is the fundamental solution of a bi-harmonic equation and can be shown as [Young, Chiu, Fan, Tsai and Lin (2006)]

$$G = \frac{-1}{8\pi} r^2 \ln(r), \tag{13}$$

where $r = \|\mathbf{x}-\mathbf{s}\|$ is the Euclidean distance between field node $\mathbf{x}$ and source node $\mathbf{s}$. Consequently, the Stokeslets can be found by substituting Eq. (13) to Eq. (11),

$$\begin{bmatrix} g_1^u & g_2^u & 0 \\ g_1^v & g_2^v & 0 \\ g_1^p & g_2^p & 0 \end{bmatrix} = \begin{bmatrix} -\frac{\partial^2}{\partial y^2} & \frac{\partial^2}{\partial x \partial y} & \left(\frac{\partial}{\partial x}\right)\nabla^2 \\ \frac{\partial^2}{\partial x \partial y} & -\frac{\partial^2}{\partial x^2} & \left(\frac{\partial}{\partial y}\right)\nabla^2 \\ \left(\frac{\partial}{\partial x}\right)\nabla^2 & \left(\frac{\partial}{\partial y}\right)\nabla^2 & \nabla^2\nabla^2 \end{bmatrix} \begin{bmatrix} G & 0 & 0 \\ 0 & G & 0 \\ 0 & 0 & 0 \end{bmatrix}. \tag{14}$$

The fundamental solutions of the Stokes equations are singular such that the sources in the MFS have to be located on fictitious boundary, which is out of the computational domain.

In order to overcome the controversial fictitious boundary of sources, the following non-singular general solution of bi-harmonic differential operator [Chen, Fu and Jin (2010)] is adopted to replace Eq. (13),

$$G^{ns} = r^2 e^{-c\left((x-s_x)^2-(y-s_y)^2\right)} \cos\left(2c(x-s_x)(y-s_y)\right), \tag{15}$$

where c is the shape parameter and have to be determined manually. In this paper, we tracked the minimum average residual of the linear system to determine the optimal shape parameter. By substituting Eq. (15) to Eq. (11), we can have the following non-singular general solutions for two-dimensional Stokes equations,

$$\begin{bmatrix} g_1^{u,ns} & g_2^{u,ns} & 0 \\ g_1^{v,ns} & g_2^{v,ns} & 0 \\ g_1^{p,ns} & g_2^{p,ns} & 0 \end{bmatrix} = \begin{bmatrix} -\frac{\partial^2}{\partial y^2} & \frac{\partial^2}{\partial x \partial y} & \left(\frac{\partial}{\partial x}\right)\nabla^2 \\ \frac{\partial^2}{\partial x \partial y} & -\frac{\partial^2}{\partial x^2} & \left(\frac{\partial}{\partial y}\right)\nabla^2 \\ \left(\frac{\partial}{\partial x}\right)\nabla^2 & \left(\frac{\partial}{\partial y}\right)\nabla^2 & \nabla^2\nabla^2 \end{bmatrix} \begin{bmatrix} G^{ns} & 0 & 0 \\ 0 & G^{ns} & 0 \\ 0 & 0 & 0 \end{bmatrix}. \tag{16}$$

Once the above non-singular general solutions of the Stokes equations, Eq. (16), are derived, two velocity components and one pressure component can be expressed

by the following equations:

$$u(\mathbf{x})=\sum_{j=1}^{n}\alpha_j^1 g_1^{u,ns}(\mathbf{x},\mathbf{s}_j)+\alpha_j^2 g_2^{u,ns}(\mathbf{x},\mathbf{s}_j)=\sum_{j=1}^{n}-\alpha_j^1\frac{\partial^2 G^{ns}(\mathbf{x},\mathbf{s}_j)}{\partial y^2}+\alpha_j^2\frac{\partial^2 G^{ns}(\mathbf{x},\mathbf{s}_j)}{\partial x\partial y}, \tag{17}$$

$$v(\mathbf{x})=\sum_{j=1}^{n}\alpha_j^1 g_1^{v,ns}(\mathbf{x},\mathbf{s}_j)+\alpha_j^2 g_2^{v,ns}(\mathbf{x},\mathbf{s}_j)=\sum_{j=1}^{n}\alpha_j^1\frac{\partial^2 G^{ns}(\mathbf{x},\mathbf{s}_j)}{\partial x\partial y}-\alpha_j^2\frac{\partial^2 G^{ns}(\mathbf{x},\mathbf{s}_j)}{\partial x^2}, \tag{18}$$

$$p(\mathbf{x})=\sum_{j=1}^{n}\alpha_j^1 g_1^{p,ns}(\mathbf{x},\mathbf{s}_j)+\alpha_j^2 g_2^{p,ns}(\mathbf{x},\mathbf{s}_j)=\sum_{j=1}^{n}\alpha_j^1\frac{\partial\nabla^2 G^{ns}(\mathbf{x},\mathbf{s}_j)}{\partial x}+\alpha_j^2\frac{\partial\nabla^2 G^{ns}(\mathbf{x},\mathbf{s}_j)}{\partial y}, \tag{19}$$

where $\left\{\alpha_j^1\right\}_{j=1}^{n}$ and $\left\{\alpha_j^2\right\}_{j=1}^{n}$ are unknown coefficients and will be acquired by enforcing the satisfactions of boundary conditions at every boundary node. n is the number of sources, which are exactly located along the physical boundary, and $\mathbf{s}_j$ is the coordinates for the j^{th} source. In addition, the solution expressions for vorticity and streamfunction can be acquired by using their definitions, Eqs. (4)-(6), and the solution expressions for these components are shown as,

$$\omega(\mathbf{x})=\sum_{j=1}^{n}\alpha_j^1\frac{\partial\nabla^2 G^{ns}(\mathbf{x},\mathbf{s}_j)}{\partial y}-\alpha_j^2\frac{\partial\nabla^2 G^{ns}(\mathbf{x},\mathbf{s}_j)}{\partial x}, \tag{20}$$

$$\psi(\mathbf{x})=\sum_{j=1}^{n}-\alpha_j^1\frac{\partial G^{ns}(\mathbf{x},\mathbf{s}_j)}{\partial y}+\alpha_j^2\frac{\partial G^{ns}(\mathbf{x},\mathbf{s}_j)}{\partial x}. \tag{21}$$

For example, if a Stokes problem with prescribed Dirichlet velocity boundary conditions is considered, we can adopt m boundary nodes, which are uniformly distributed along physical boundary. Since the non-singular general solutions of Stokes equations already satisfied the governing equations, the satisfactions of boundary conditions have to be imposed to determine the coefficients in the solution expressions. By enforcing the satisfactions of given Dirichlet velocity boundary conditions at every boundary node, a system of linear algebraic equations is yielded,

$$\bar{u}(\mathbf{x}_i)=\sum_{j=1}^{n}-\alpha_j^1\left.\frac{\partial^2 G^{ns}(\mathbf{x},\mathbf{s}_j)}{\partial y^2}\right|_{\mathbf{x}=\mathbf{x}_i}+\alpha_j^2\left.\frac{\partial^2 G^{ns}(\mathbf{x},\mathbf{s}_j)}{\partial x\partial y}\right|_{\mathbf{x}=\mathbf{x}_i}\quad i=1,2,3,.....m, \tag{22}$$

$$\bar{v}(\mathbf{x}_i) = \sum_{j=1}^{n} \alpha_j^1 \left. \frac{\partial^2 G^{ns}(\mathbf{x},\mathbf{s}_j)}{\partial x \partial y} \right|_{\mathbf{x}=\mathbf{x}_i} - \alpha_j^2 \left. \frac{\partial^2 G^{ns}(\mathbf{x},\mathbf{s}_j)}{\partial x^2} \right|_{\mathbf{x}=\mathbf{x}_i} \quad i = 1,2,3.....m, \tag{23}$$

where $\bar{u}(\mathbf{x}_i)$ and $\bar{v}(\mathbf{x}_i)$ are given velocity boundary conditions at the i^{th} boundary node. By using the collocation approach at every boundary node, a system of $2m$ linear equations with $2n$ unknowns is yielded,

$$\mathbf{A}_{(2m)\times(2n)}\mathbf{q}_{(2n)\times 1} = \mathbf{b}_{(2m)\times 1}, \tag{24}$$

where $\mathbf{A}$ is the coefficient matrix. $\mathbf{q} = \left[\alpha_1^1, \alpha_2^1, \alpha_3^1, ..., \alpha_n^1, \alpha_1^2, \alpha_2^2, \alpha_3^2, ..., \alpha_n^2\right]^T$ is the unknown vector where the superscript T denotes the transpose of the matrix. $\mathbf{b} = [\bar{u}(\mathbf{x}_1), \bar{u}(\mathbf{x}_2), ..., \bar{u}(\mathbf{x}_m), \bar{v}(\mathbf{x}_1), \bar{v}(\mathbf{x}_2), ..., \bar{v}(\mathbf{x}_m)]^T$ is the vector of given boundary conditions. The unknown vector can be acquired by solving the above system of linear algebraic equations. Once the unknown coefficients are obtained, the velocity components, pressure, vorticity and streamfunction at any position can be acquired by simple summation in Eqs. (17)-(21).

Because the linear system in the BKM is ill-conditioned [Wang, Chen and Jiang (2010)], in this study we used the least-squares method to reduce this problem by setting $m = 2n$. Namely, the number of boundary nodes is twice the number of sources. Furthermore, the optimal shape parameter c of Eq. (15) is determined by tracing the minimum of the average residual $\frac{\|\mathbf{Aq}-\mathbf{b}\|}{2m}$. A range of c and the increment of c are defined manually, so a vector of c can be acquired. For each c, the numerical procedure of Eqs. (22)-(24) are implemented and then a corresponding value of average residual can be obtained. When everyone of the c vector and their corresponding average residuals are calculated, the optimal c can be determined according to the minimum among those average residuals. The optimal value of c is used to calculate the distributions of physical values inside computational domain. From the above descriptions, it can be found that the numerical procedure of the BKM is very simple once the non-singular general solutions of the Stokes equations are derived. Three numerical examples were provided in the next section to verify the merits of the BKM for numerical solutions of two-dimensional Stokes flows.

4 Numerical Results and Comparisons

In this paper, the non-singular general solutions of two-dimensional Stokes equations are derived to form the solution expressions of the BKM. The sources of the BKM can be located along the physical boundary, such that the controversial fictitious boundary for sources in the MFS can be avoided. In addition, the least-squares method is used to reduce the problem of ill-conditioned matrix in the BKM. The optimal shape parameter in the non-singular general solutions was determined according to the minimum of the average residual. In the following subsections, the

numerical results and comparisons of three examples of Stokes flows were provided to validate the accuracy and the simplicity of the BKM.

4.1 Example 1

The first example in this paper is the Stokes flow in a lid-driven square cavity and the computational domain is a unit square. Unit positive x-directional velocity is imposed along the top lid while the no-slip boundary condition is given along the other three sides of the cavity. The schematic diagram of the square cavity is shown in Fig. 1(a), as 200 boundary nodes are uniformly distributed along the boundary, which is demonstrated in Fig. 1(b). In order to achieve accurate and stable numerical results, the profiles of the variation of average residual with respect to shape parameter are depicted in Fig. 2 when the number of boundary nodes is set as 200, 400 and 800. In our test, the study range for shape parameter c is $0 < c \leq 20$ and 200 different shape parameters are uniformly determined in this range. For each c, the numerical procedures of the proposed BKM, Eqs. (22)-(24), are implemented and a average residual is obtained. From this figure, we can find a minimum average residual at every profile and the optimal shape parameter is then determined at the minimum average residual. According to the results in this figure, the optimal shape parameter is equal to 16, 16.5 and 17 when 200, 400 and 800 boundary nodes are adopted.

We used 2401 interior nodes to plot the distributions of flow field inside the computational domain. The distributions of x-directional velocity, y-directional velocity, velocity vector, pressure and streamlines are illustrated in Figs. 3(a)-3(e). Since the results by using m=200 are almost identical to those obtained by using m=400 and m=800, only the solutions for m=200 are provided in this paper for simplicity. The numerical results are in good agreements with those obtained by the RBFCM [Young, Jane, Lin, Chiu and Chen (2004)], and the MFS [Young, Jane, Fan, Murugesan and Tsai (2006)]. A main circulation moving in the clockwise direction near the center of cavity is obvious from the distributions of velocity vector and streamlines in Figs. 3(c) and 3(e). In order to carefully examine the accuracy of results, the profiles of x-directional velocity along the central vertical axis and the y-directional velocity along the central horizontal axis are depicted in Figs. 4(a)-4(b). The numerical results of the BKM by using 200, 400 and 800 boundary nodes are compared well with the solutions by the RBFCM [Young, Jane, Lin, Chiu and Chen (2004)] in these figures. The accuracy and the consistency of the proposed BKM are validated from these figures. Besides, the comparisons in Fig. 4 also verified that the proposed scheme for determining the optimal shape parameter from the minimum average residual is useful.

In 2012, Barrero-Gil proposed a numerical technique for dealing with the singular-

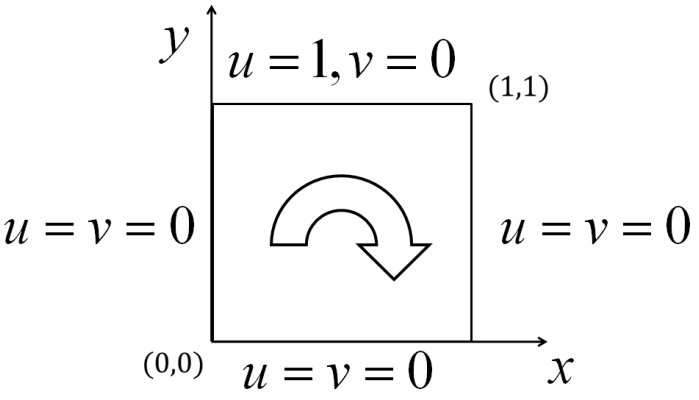

(a)

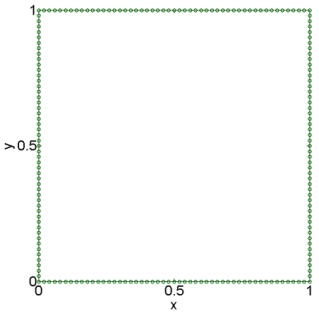

(b)

Figure 1: (a) The schematic diagram of lid-driven square cavity and (b) distribution of boundary nodes.

ity of the MFS when the fictitious boundary is located exactly along the physical boundary. The singular entries of the coefficient matrix are replaced by averaging the influences of a group of auxiliary Stokeslets near each singularity, so more efforts for calculating the coefficient matrix should be paid and the resultant system of linear algebraic equations have to be solved only once. However, in our proposed BKM, the system of linear algebraic equations should be analyzed several times in order to find the optimal shape parameter. From the viewpoint of computational efficiency, the computational cost in the proposed BKM is higher than the modified MFS [Barrero-Gil (2012)] due to the direct-searching of optimal shape parameter. Therefore, more efficient way for determining the optimal shape parameter should be researched in the future.

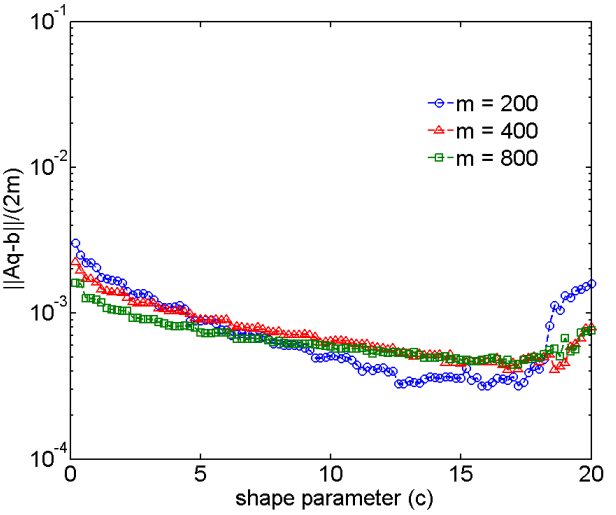

Figure 2: Profiles of average residual of linear system with respect to different shape parameters.

4.2 Example 2

The second example is the lid-driven circular cavity, which is depicted in Fig. 5(a). A tangential velocity with unit magnitude in counterclockwise direction is imposed along the upper half boundary, as the no-slip boundary condition is given along the bottom half boundary. From the imposed boundary conditions, we can expect that a main circulation moving in the counterclockwise direction will appear near the center of the cavity. In this example, we adopted 100 boundary nodes, which are demonstrated in Fig 5(b), for numerical simulation. When 100, 200, 400 and 800 boundary nodes are adopted, there will appear a minimum average residual for every profile in Fig. 6 and then the optimal shape parameter can be determined. The optimal shape parameter is equal to 2.5, 3, 3 and 3 while 100, 200, 400 and 800 boundary nodes are used.

The numerical results of x-directional velocity, y-directional velocity, velocity vector, vorticity and streamlines are depicted in Figs. 7(a)-7(e). Since using these four different numbers of boundary nodes can acquire very similar solutions, we only provide the results by using 100 boundary nodes. Due to the imposed boundary conditions, the distributions of x-directional velocity and y-directional velocity in Figs. 7(a)-7(b) are symmetric and anti-symmetric (skew-symmetric) with respect to y axis. As we expected, a main circulation appeared near the center of cav-

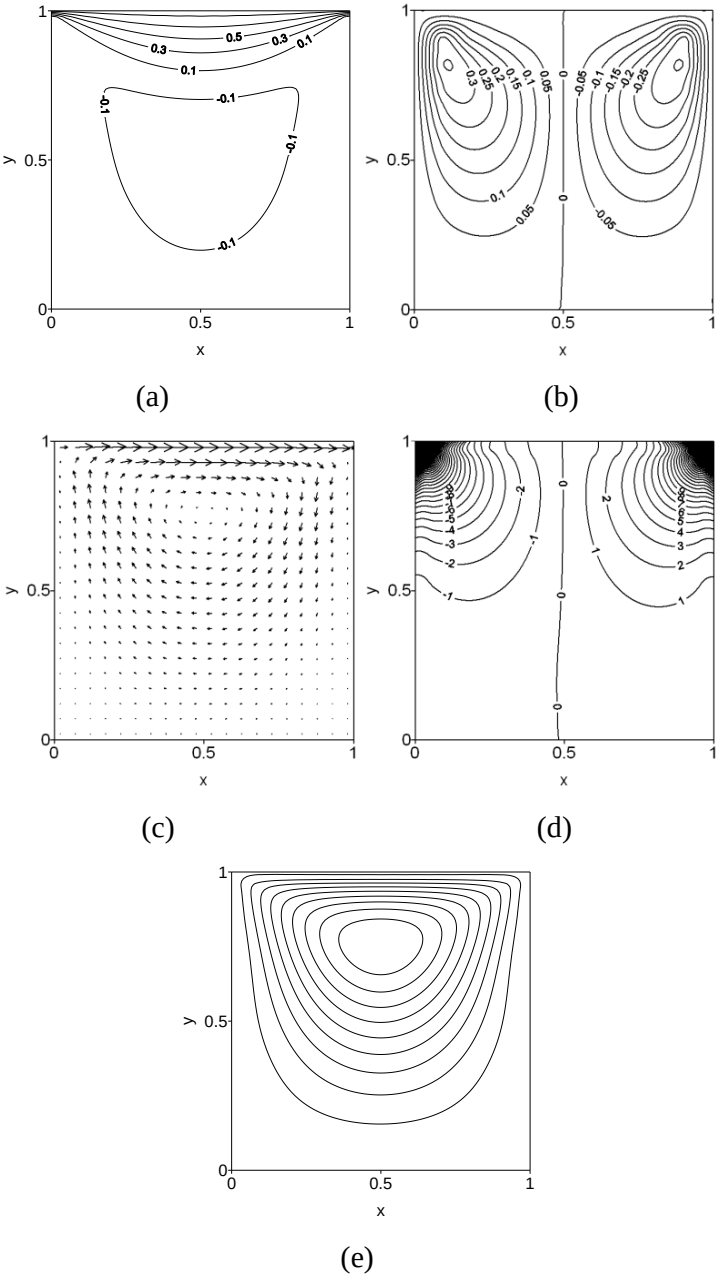

Figure 3: Distributions of (a) x-directional velocity, (b) y-directional velocity, (c) velocity vector, (d) pressure and (e) streamlines.

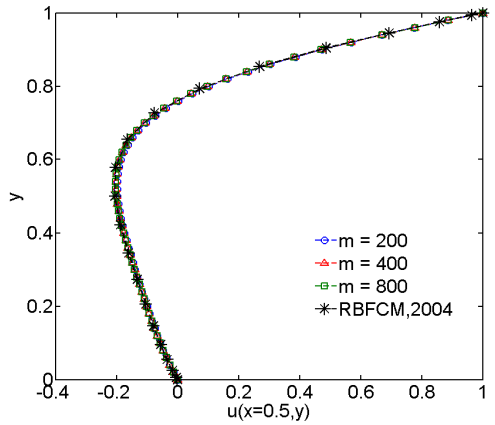

(a)

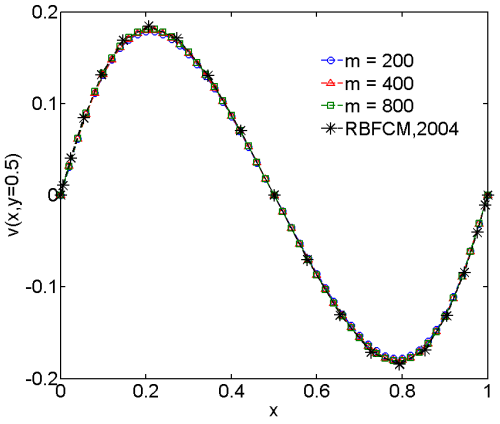

(b)

Figure 4: Profiles of (a) x-directional velocity along central vertical axis and (b) y-directional velocity along central horizontal axis.

ity in Fig. 7(c). The provided results are in good agreements with the solutions by the RBFCM [Young, Jane, Lin, Chiu and Chen (2004)], one kind of domain-type meshless methods. Furthermore, the profiles of x-directional velocity along the central vertical axis and the y-directional velocity along the central horizontal axis are demonstrated in Figs. 8(a)-(b).The numerical results by adopting different numbers of boundary nodes are almost identical to each other and they are very similar to the solutions by using dual reciprocity BEM [Young, Tsai, Eldho and

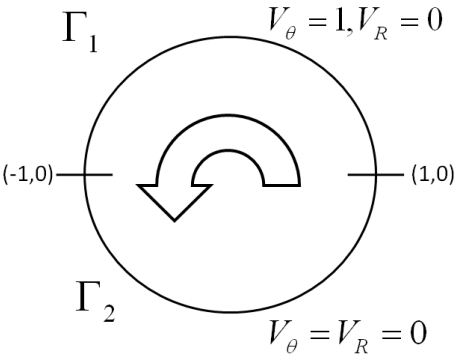

(a)

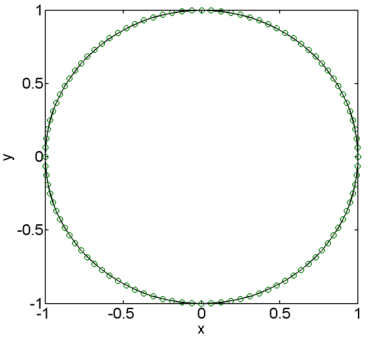

(b)

Figure 5: (a) The schematic diagram of lid-driven circular cavity and (b) distribution of boundary nodes.

Cheng (2002)]. The accuracy of the proposed BKM for numerical solutions of Stokes flows are validated from the provided numerical results in this example. It is obvious that profiles in Fig. 6 are near flat when shape parameter c is smaller than 4. Similar with the solutions in Fig. 8, the results along two central axes are depicted in Fig. 9 by using different shape parameters. To adopt $c = 1$, $c = 2$ and $c = 3$ can acquire similar level of average residuals, so their results are very close to each other and extremely accurate. Conversely, the profiles for $c = 7$ in Fig. 9 are very different from others since the average residual for $c = 7$ is quite larger than those for $c = 1$, $c = 2$ and $c = 3$. Hence, it is also verified that the optimal shape parameter of the non-singular general solutions can be determined by the proposed technique.

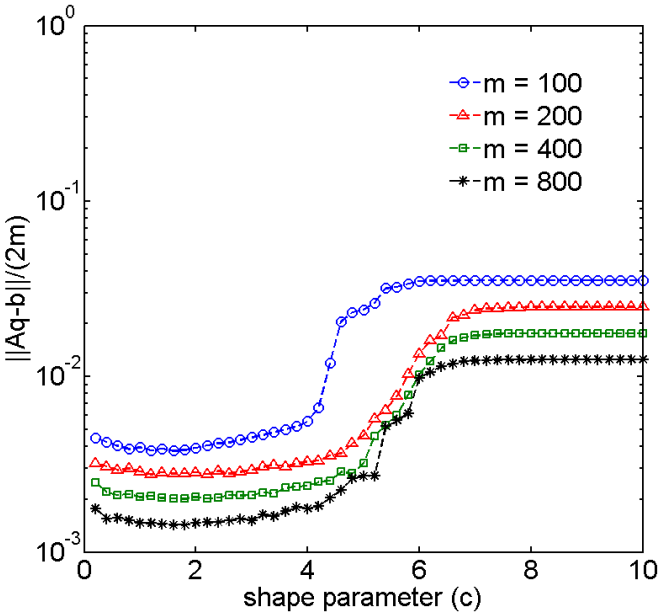

Figure 6: Profiles of average residual of linear system with respect to different shape parameters.

4.3 Example 3

The third example is the lid-driven rectangular cavity with wave-shaped bottom, which is depicted in Fig. 10(a). The function to describe the bottom shape and the given boundary conditions are shown in Fig. 10(a). In this case, we adopted 561 boundary nodes, distributed along the physical domain and demonstrated in Fig. 10(b). The profile of the average residual of the linear system with respect to shape parameter is given in Fig. 11 and then the optimal shape parameter is equal to 3 according to this figure. We used 938 interior nodes to show the results of x-directional velocity, velocity vector, vorticity and streamlines in Figs. 12(a)-12(d). From these results, a main circulation inside the cavity can be easily found. Besides, the flow pattern influenced by the bottom shape is obvious and these numerical results are in good agreements with the solutions by using the MFS [Young, Jane, Fan, Murugesan and Tsai (2006)]. The accuracy and the simplicity of the proposed BKM are verified from these provided numerical results and comparisons.

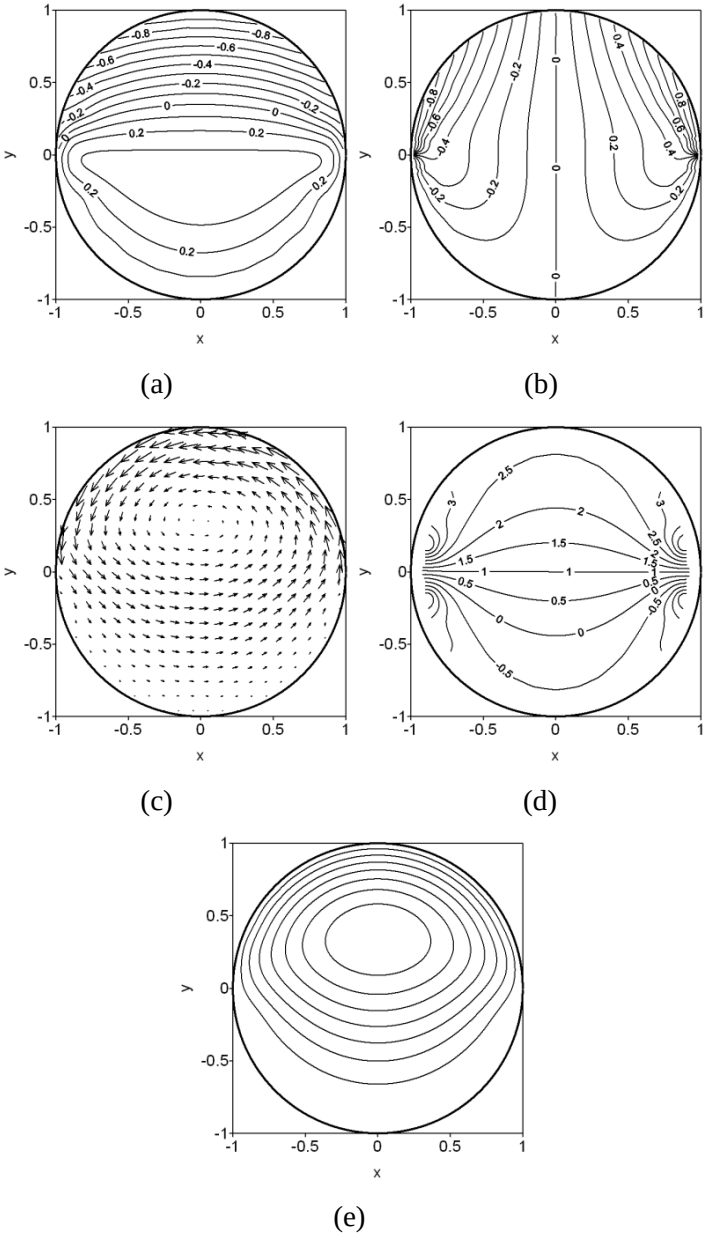

Figure 7: Distributions of (a) x-directional velocity, (b) y-directional velocity, (c) velocity vector, (d) vorticity and (e) streamlines.

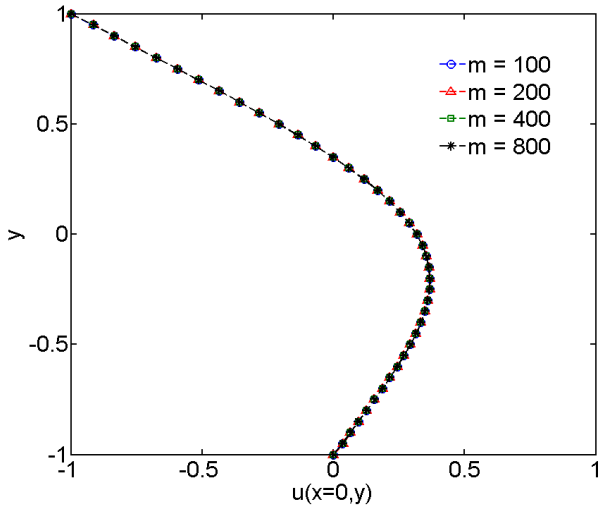

(a)

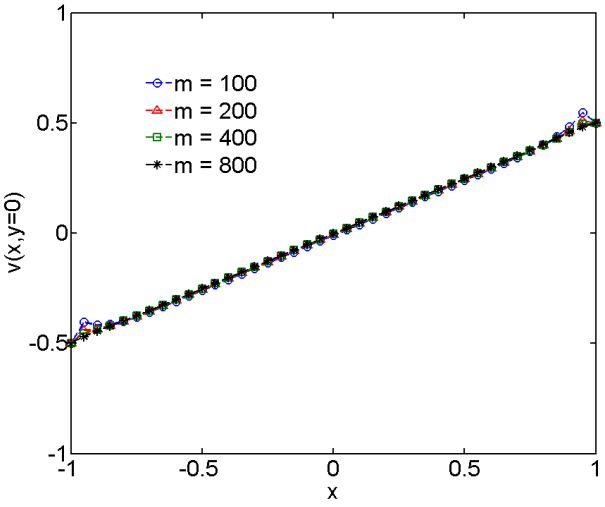

(b)

Figure 8: Profiles of (a) x-directional velocity along central vertical axis and (b) y-directional velocity along central horizontal axis.

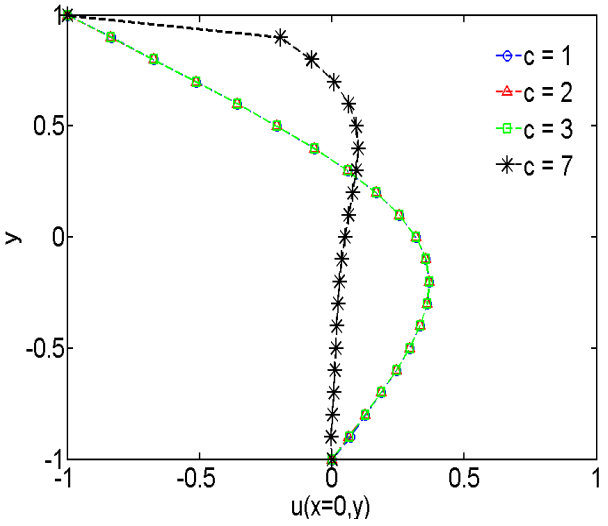

(a)

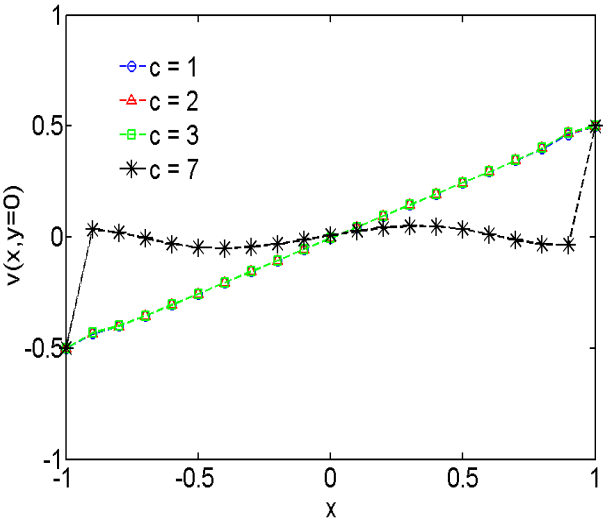

(b)

Figure 9: Profiles of (a) x-directional velocity along central vertical axis and (b) y-directional velocity along central horizontal axis by adopting different shape parameters.

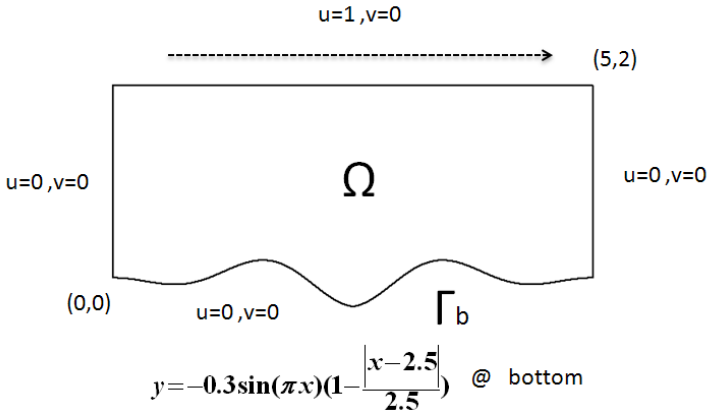

(a)

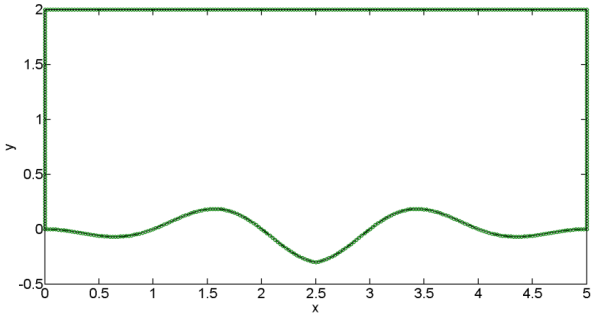

(b)

Figure 10: (a) The schematic diagram of lid-driven rectangular cavity with wave-shaped bottom and (b) distribution of boundary nodes.

5 Conclusions and Discussions

The BKM, a promising boundary-type meshless method, was adopted to analyze the two-dimensional Stokes flows in this paper. The BKM is truly free from mesh generation and numerical quadrature, as well as only boundary nodes are necessary during its numerical implementation. In contrast to fictitious boundary of the MFS, the sources in the BKM can be exactly located on the physical boundary. The non-singular general solutions of the two-dimensional Stokes equations, which were derived by the Hormander operator decomposition method in this paper, are adopted to express the numerical solutions of the BKM. Thus, the unknown coefficients in the solution expressions can be acquired by enforcing the satisfactions of

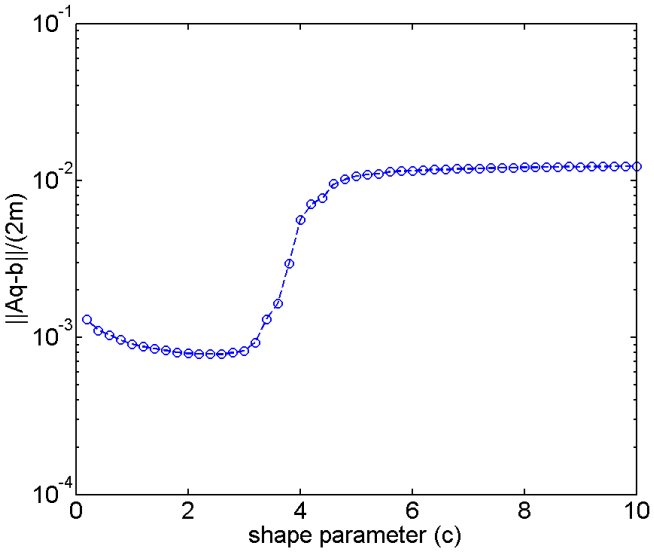

Figure 11: Profiles of average residual of linear system with respect to different shape parameters.

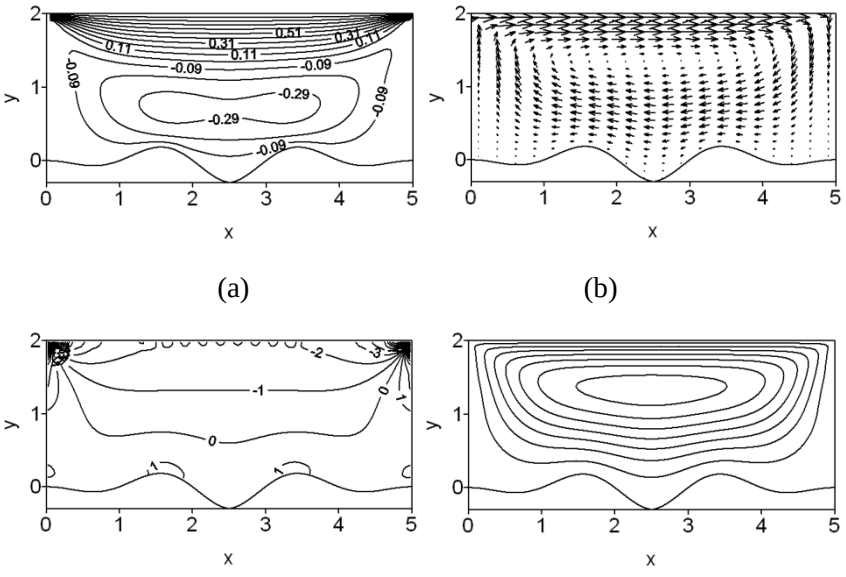

Figure 12: Distributions of (a) x-directional velocity (b) velocity vector, (c) vorticity and (d) streamlines.

boundary conditions via a collocation approach. The least-squares method, which means that the number of boundary nodes is greater than the number of sources, is adopted to reduce the problem of ill-conditioned matrix. In addition, the optimal shape parameter in the non-singular general solutions was determined by tracking the minimum average residual of the resultant linear system.

Three numerical examples were provided to validate the accuracy, the consistency and the simplicity of the proposed BKM. The accurate numerical results were acquired by using very few boundary nodes. In addition, the numerical results in these three examples by adopting the BKM are compared well with those obtained by the RBFCM, the MFS and the dual reciprocity BEM. The proposed BKM for numerical solutions of Stokes equations and the way for deriving the non-singular general solutions will be directly extended to Stokes problems in multiply-connected domains and three-dimensional Stokes problems in the near future. In addition, although the way for acquiring the optimal shape parameter, c, in this paper is workable, we will focus our future research on developing more efficient scheme to determine this shape parameter.

References

Alves, C. J. S.; Silvestre, A. L. (2004): Density results using Stokeslets and a method of fundamental solutions for the Stokes equations. *Engineering Analysis with Boundary Elements,* vol. 28, pp. 124552

Barrero-Gil, A. (2012): The method of fundamental solutions without fictitious boundary for solving Stokes problems. *Computers & Fluids*, vol. 62, pp. 8690

Barrero-Gil, A. (2013): The method of fundamental solutions without fictitious boundary for axissymmetric Stokes problems. *Engineering Analysis with Boundary Elements*, vol. 37, pp. 393400

Benito, J. J.; Urena, F.; Gavete, L.; Alonso, B. (2008): Application of the generalized finite difference method to improve the approximated solution of pdes. *CMES: Computer Modeling in Engineering & Sciences*, vol. 38, pp. 39-58.

Canelas, A.; Sensale, B. (2010): A boundary knot method for harmonic elastic and viscoelastic problems using a single-domain approach. *Engineering Analysis with Boundary Elements*, vol. 34, pp. 845-55.

Chan, H. F.; Fan, C. M. (2013): The local radial basis function collocation method for solving two-dimensional inverse Cauchy problems. *Numerical Heat Transfer, Part B: Fundamentals*, vol. 63, pp. 284-303.

Chan, H. F.; Fan, C. M.; Kuo, C. W. (2013): Generalized finite difference method for solving two-dimensional nonlinear obstacle problem. *Engineering Analysis*

with Boundary Elements, vol. 37, pp. 1189-96.

Chen, W. (2002): Symmetric boundary knot method. *Engineering Analysis with Boundary Elements*, vol. 26, pp. 487-94.

Chen, J. T.; Chang, M. H.; Chen, K. H.; Chen, I. L. (2002): Boundary collocation method for acoustic eigenanalysis of three-dimensional cavities using radial basis function. *Computational Mechanics*, vol. 29, pp. 392-408.

Chen, J. T.; Chang, M. H.; Chen, K. H.; Lin, S. R. (2002): The boundary collocation method with meshless concept for acoustic eigenanalysis of two-dimensional cavities using radial basis function. *Journal of Sound and Vibration*, vol. 257, pp. 667-711.

Chen, C. S.; Fan, C. M.; Wen, P. H. (2011): The method of approximate particular solutions for solving elliptic problems with variable coefficients. *International Journal of Computational Methods*, vol. 8, pp. 545-59.

Chen, C. S.; Fan, C. M.; Wen, P. H. (2012): The method of approximate particular solutions for solving certain partial differential equations. *Numerical Methods for Partial Differential Equations*, vol. 28, pp. 506-22.

Chen, W.; Fu, Z. J.; Jin, B. T. (2010): A truly boundary-only meshfree method for inhomogeneous problems based on recursive composite multiple reciprocity technique. *Engineering Analysis with Boundary Elements*, vol. 34, pp. 196-205.

Chen, W.; Fu, Z. J.; Wei X. (2009): Potential problems by singular boundary method satisfying moment condition. *CMES: Computer Modeling in Engineering & Sciences*, vol. 54, pp. 65-85.

Chen, W.; Gu, Y. (2012): An improved formulation of singular boundary method. *Advances in Applied Mathematics and Mechanics*, vol, 4, pp. 543-58.

Chen, W.; Hon, Y. C. (2003): Numerical investigation on convergence of boundary knot method in the analysis of homogeneous Helmholtz, modified Helmholtz, and convection-diffusion problems. *Computer Methods in Applied Mechanics and Engineering*, vol. 192, pp. 1859-75.

Chen, J. T.; Hsiao, C. C.; Leu, S. Y. (2008): A new method for Stokes problems with circular boundaries using degenerate kernel and Fourier series. *International Journal for Numerical Methods in Engineering*, vol. 74, pp. 1955-1987.

Chen, J. T.; Lee, Y. T.; Yu, S. R.; Shieh, S. C. (2009): Equivalence between the Trefftz method and the method of fundamental solution for the annular Green's function using the addition theorem and image concept. *Engineering Analysis with Boundary Elements*, vol. 33, pp. 678-88.

Chen, W.; Shen, L. J.; Shen, Z. J.; Yuan, G. W. (2005): Boundary knot method for Poisson equations. *Engineering Analysis with Boundary Elements*, vol. 29, pp.

756-60.

Chen, W.; Tanaka, M. (2002): A meshless, integral-free, and boundary-only RBF technique. *Computers & Mathematics with Applications*, vol. 43, pp. 379-91.

Fan, C. M.; Chan, H. F.; Kuo, C. L.; Yeih, W. (2012): Numerical solutions of boundary detection problems using modified collocation Trefftz method and exponentially convergent scalar homotopy algorithm. *Engineering Analysis with Boundary Elements*, vol. 36, pp. 2-8.

Fan, C. M.; Chien, C. S.; Chan, H. F.; Chiu, C. L. (2013): The local RBF collocation method for solving the double-diffusive natural convection in fluid-saturated porous media. *International Journal of Heat and Mass Transfer*, vol. 57, pp. 500-3.

Fan C. M.; Huang, Y. K.; Li, P. W.; Chiu, C. L. (2014): Application of the generalized finite-difference method to inverse biharmonic boundary-value problems. *Numerical Heat Transfer, Part B: Fundamentals*, vol. 65, pp. 129-54.

Fu, Z. J.; Chen, W.; Chen, J. T.; Qu, W. Z. (2014): Singular boundary method: three regularization approaches and exterior wave applications. *CMES: Computer Modeling in Engineering & Sciences*, vol. 99, pp. 417-43.

Hon, Y. C.; Chen, W. (2003): Boundary knot method for 2D and 3D Helmholtz and convection-diffusion problems under complicated geometry. *International Journal for Numerical Methods in Engineering*, vol. 56, pp. 1931-48.

Jin, B.; Zheng, Y. (2005a): Boundary knot method for some inverse problems associated with the Helmholtz equation. *International Journal for Numerical Methods in Engineering*, vol. 62, pp. 1636-51.

Jin, B.; Zheng, Y. (2005b): Boundary knot method for the Cauchy problem associated with the inhomogeneous Helmholtz equation. *Engineering Analysis with Boundary Elements*, vol. 29, pp. 925-35.

Karageorghis, A.; Lesnic, D; Marin, L. (2014): Regularized collocation Trefftz method for void detection in two-dimensional steady-state heat conduction problems. *Inverse Problems in Science and Engineering*, vol. 22, pp. 395-418.

Ku, C. Y. (2014): On solving three-dimensional Laplacian problems in a multiply connected domain using the multiple scale Trefftz method. *CMES: Computer Modeling in Engineering & Sciences*, vol. 98, pp. 509-41.

Lin, J.; Chen, W.; Chen, C. S.; Jiang, X. R. (2013): Fast boundary knot method for solving axisymmetric Helmholtz problems with high wave number. *CMES: Computer Modeling in Engineering & Sciences*, vol. 94, pp. 485-505.

Rashed, Y. F. (2002): Tutorial 5: fundamental solutions: II-matrix operators. *Boundary Element Communications*, vol. 13, pp. 35-45.

Tsai, C. C.; Hsu, T. W. (2011): A meshless numerical method for solving slow

mixed convections in containers with discontinuous boundary data. *International Journal for Numerical Methods in Fluids*, vol. 66, pp. 377-402.

Tsai, C. C.; Young, D. L. (2013): Using the method of fundamental solutions for obtaining exponentially convergent Helmholtz eigensolutions. *CMES: Computer Modeling in Engineering & Sciences*, vol. 94, pp. 175-205.

Vertnik, R.; Sarler, B. (2009): Solution of incompressible turbulent flow by a mesh-free method. *CMES: Computer Modeling in Engineering & Sciences*, vol. 44, pp. 65-95.

Wang, F.; Chen, W.; Jiang, X. (2010): Investigation of regularized techniques for boundary knot method. *International Journal for Numerical Methods in Biomedical Engineering*, vol. 26, pp. 1868-77.

Young, D. L.; Chen, C. W.; Fan, C. M.; Murugesan K.; Tsai, C. C. (2005): The method of fundamental solutions for Stokes flow in a rectangular cavity with cylinders. *European Journal of Mechanics–B/Fluids*, vol. 24, pp. 703-16.

Young, D. L.; Chiu, C. L.; Fan, C. M.; Tsai, C. C.; Lin, Y. C. (2006): Method of fundamental solutions for multidimensional Stokes equations by the dual-potential formulation. *European Journal of Mechanics–B/Fluids*, vol. 25, pp. 877-93.

Young, D. L.; Jane, S. J.; Fan, C. M.; Murugesan K.; Tsai, C. C. (2006): The method of fundamental solutions for 2D and 3D Stokes problems. *Journal of Computational Physics*, vol. 211, pp. 1-8.

Young, D. L.; Jane, S. C.; Lin, C. Y.; Chiu, C. L.; Chen, K. C. (2004): Solutions of 2D and 3D Stokes laws using multiquadrics method. *Engineering Analysis with Boundary Elements*, vol. 28, pp. 123343.

Young, D. L.; Tsai, C. C.; Eldho, T. I.; Cheng, A. H. D. (2002): Solution of Stokes flow using an iterative DRBEM based on compactly-supported, positive-definite radial basis function. *Computers and Mathematics with Applications*, vol. 43, pp.607-19.

Zeb, A.; Elliott, L.; Ingham, D. B.; Lesnic, D. (1998): The boundary element method for the solution of Stokes equations in two-dimensional domains. *Engineering Analysis with Boundary Elements,* vol. 22, pp. 31726.

Zhang, J. Y.; Wang, F. Z. (2012): Boundary knot method: an overview and some novel approaches. *CMES: Computer Modeling in Engineering & Sciences*, vol. 88, pp. 141-52.

Zheng, K. H.; Ma, H. W. (2012): Combination of the boundary knot method with analogy equation method for nonlinear problems. *CMES: Computer Modeling in Engineering & Sciences*, vol. 87, pp. 225-38.